Borneo Journal of Resource Science and Technology (2024), 14(2): 81-97
DOI: https:doi.org/10.33736/bjrst.7417.2024

Morphology and Molecular Characterisation of *Karenia mikimotoi* (Dinophyceae) from Sabah Malaysian Borneo, with a Focus on the Second Internal Transcribed Spacer (ITS2) of Ribosomal RNA gene

SHERYL UNCHA ANDREW CHIBA[1], SING TUNG TENG*[1], SAMSUR MOHAMAD[1], NURSYAHIDA ABDULLAH[1], ING KUO LAW[1], PO TEEN LIM[2] & CHUI PIN LEAW[2]

[1]Faculty of Resource Science and Technology, Universiti Malaysia Sarawak, Kota Samarahan, 94300 Sarawak, Malaysia; [2]Bachok Marine Research Station, Institute of Ocean and Earth Sciences, University of Malaya, 16310 Bachok, Kelantan, Malaysia
* Corresponding author: tsteng@unimas.my
Received: 17 July 2024 Accepted: 8 November 2024 Published: 31 December 2024

ABSTRACT

The first recorded bloom of *Karenia mikimotoi* (initially *Gymnodinium mikimotoi*) occurred off the coast of Japan in 1934, causing mass mortality of shellfish and fish. This event highlighted the devastating impact of *K. mikimotoi* blooms and marked a turning point in harmful algal bloom (HAB) research, driving studies on its identification, biology, toxicology, and effects on marine life and ecosystems. The past reported bloom events in Southeast Asia have raised public concerns, leading to further investigation into the occurrence and geographical distribution of *K. mikimotoi* in the region. As of yet, there is no recorded evidence of *K. mikimotoi* blooms in Malaysian waters. This prompt the investigation of the occurrence and distribution of *K. mikimotoi* in Malaysia, and this study represent the first record of *K. mikimotoi* in Malaysian waters. In this study, clonal cultures of *K. mikimotoi* isolated from Sepanggar Bay, Sabah were examined using light microscopy (LM) and scanning electron microscopy (SEM) to observe its morphological features. Cells of *K. mikimotoi* from Malaysian Borneo exhibited a typical dorso-ventrally flattened body with bi-lobed and linear apical grooves on the cell apex. Molecular characterisation of the strains based on the internal transcribed spacer (ITS) region and large-subunit (LSU) ribosomal DNA revealed close phylogenetic relationships with other strains of *K. mikimotoi* from other regions, forming a monophyletic clade that positioned as sister to *K. brevis*, supporting the species identity of *K. mikimotoi*. The secondary structure of the ITS2 RNA transcript revealed a universal structure with four major helices. Structural comparison between *K. mikimotoi* and its relatives revealed four to six hemi-compensatory base changes. The results demonstrated the efficacy of ITS2 secondary structure information in delimiting species in *Karenia*. The detailed morphology and molecular characteristics of *K. mikimotoi* were revealed, for the first time, from the coastal waters of Malaysian Borneo.

Keywords: Kareniaceae, Malaysia, phylogeny, ribosomal RNA gene, rRNA transcript

INTRODUCTION

The genus *Karenia* G. Hansen & Moestrup, 2000 (order: Gymnodiniales; family: Kareniaceae) is a group of athecate dinoflagellates that contribute to the harmful algal bloom (HAB) phenomena (Cen *et al*., 2020). Some species of *Karenia* have been reported to cause mass fatalities of marine animals and massive fish mortality, leading to significant economic losses in marine and coastal aquaculture (Davis, 1948; Gunter *et al*., 1948; Flewelling *et al*., 2005; Li *et al*., 2019). The genus *Karenia* also poses threats to public health through neurotoxic shellfish poisoning (NSP) and respiratory illnesses (Watkins *et al*., 2008; Heil & Steidinger, 2009; Hoagland *et al*., 2009).

The lack of comprehensive taxonomical study for *Karenia* species has become critically important since the discovery of red tides that killed marine life. Recently, a new *Karenia* species called *K. hui* had been described from China (Cen *et al*., 2024). Over three decades, the taxonomical classification of the genus *Karenia* has progressed significantly, and as of now, the genus *Karenia* is consists of eleven recognised species namely *Karenia asterichroma, K. bicuneiformis* (synonym: *K. bidigitata), K. brevis*, *K. brevisulcata*, *K. concordia, K. cristata*, *K. hui*, *K. longicanalis* (synonym: *K.*

umbella), *K. mikimotoi*, *K. papilionacea*, and *K. selliformis* (Guiry and Guiry, 2023; Cen *et al*., 2024).

Naked dinoflagellates of genus *Karenia* were previously classified under genus *Gymnodinium* before genus *Karenia* was established (Bergholtz *et al*., 2006; Caruana & Amzil, 2018). The historical taxonomic of *K. mikimotoi* became a state of turmoil, particularly after the strain isolated from European waters was identified as *Gyrodinium* cf. *aureoleum* (Hulburt, 1957; Gentien, 1998). Strains discovered from different areas of Japan were named as *Gymnodinium* sp., *G*. sp. 1 and *G*. type-'65 but were later re-assessed and re-described as *K. mikimotoi* (Fukuyo *et al*., 2002). In 1984, additional strains from Japan were named *Gymnodinium nagasakiense* owing to the dissimilar morphology traits as *G. mikimotoi* under light microscopy (Takayama & Adachi, 1984), and *Gyrodinium nagasakiense*, based on cingular displacement with European *G*. cf. *aureolum* (Tangen, 1977; Takayama & Adachi, 1984; Partensky *et al*., 1988). Molecular studies later confirmed that *Gymnodinium nagasakiense* and *Gyrodinium nagasakiense* were actually identical to *Gymnodinium mikimotoi* (Hansen *et al*., 2000). Comprehensive morphological, molecular, and pigment analyses on the European *G*. cf. *aureolum* and *G. mikimotoi* were performed and had reached a consensus that European *G*. cf. *aureolum* was conspecific with *G. mikimotoi* (Hansen *et al*., 2000; Tang *et al*., 2008). A re-evaluation by Daugbjerg *et al*. (2000) highlighted the presence of a straight apical groove as a unique feature of all *Karenia* species which was morphologically distinct than that of *Gymnodinium* sensu stricto, thus, separating *Karenia* species from genus *Gymnodinium.* Consequently, *Gymnodinium mikimotoi* was reclassified as *Karenia mikimotoi* (Daugbjerg *et al*., 2000).

K. mikimotoi (formerly known as *Gymnodinium mikimotoi*) was described from Gokasho Bay, Japan (Oda, 1935). The name "mikimotoi" was given to this species in reference to Mikimoto Kōkichi, the "Pearl King" who was known inside and outside the Japanese empire for pearl cultivation in Gokasho Bay (Eunson, 1955; Ericson, 2016). Over the course of more than 80 years, this HAB-forming dinoflagellate species has caused mass mortalities in marine life worldwide, mainly in the coastal waters of Europe and Asia (Li *et al*., 2019).

In the Asian region, blooms of *K. mikimotoi* have been reported since the 1930s. Several areas in Japan have documented the blooms of this species (Oda, 1935; Takayama & Adachi, 1984; Yanagi *et al*., 1995; Matsuyama *et al*., 1999; Siswanto *et al*., 2013; Li *et al*., 2019). In Gokasho Bay, Honshu, Japan, the *K. mikimotoi* blooms in 1934 caused mortalities of fish and shellfish (Oda, 1935). In Omura Bay, Nagasaki, a *K. mikimotoi* bloom was associated with fish and shellfish deaths in 1965 (Takayama & Adachi, 1984). In Suo-Nada and Iyo-Nada, Japan, a *K. mikimotoi* bloom in 1985 caused significant damage to the fisheries, with financial losses exceeding 10 million USD (Yanagi *et al*., 1995). From 1981 to 1985, *K. mikimotoi* was reported in Korean coastal waters (Park *et al*., 2013). In 1989, a bloom of *K. mikimotoi* associated with a fish kill event occurred in Indian waters (D'Silva *et al*., 2012). In the Bolinao-Anda area, Pangasinan province in the Philippines, high biomass of *K. mikimotoi* was occasionally reported, but no fish kills were observed (Yñiguez *et al*., 2021). In 1998, *K. mikimotoi* blooms was reported in Hong Kong waters (Lu & Hodgkiss, 2004), this red tide caused significant losses to about two-thirds (estimated 1000 out of 1500) of mariculture farms, with an estimated financial loss of 315 million HKD (40 million USD). Following the first bloom in the coastal waters of China, the bloom areas of *K. mikimotoi* were observed to spread from Guangdong province to Tianjin city, and the provinces of Zhejiang, Fujian, Hebei, and Jiangsu (Baohong *et al*., 2021). Blooms of *K. mikimotoi* in China have become frequent in the East China Sea, including the Changjiang River estuary and the coastal areas of Zhejiang and Fujian Provinces, almost every year since 2002 (Li *et al*., 2017). In 2011 and 2014, *K. mikimotoi* caused patches of water discoloration along the east Johor Strait, Singapore (Leong *et al*., 2015).

Within the Southeast Asian region, Vietnam, Singapore, and Philippines are the countries that have reported the occurrences of *K. mikimotoi* (Larsen & Nguyen, 2004; Leong *et al*., 2015; Azanza and Benico, 2017; Yñiguez *et al*., 2021). The presence of the species was first reported in Vietnamese coastal waters in a sampling survey in 1999. As reported by Leong *et al*. (2015), a

high biomass of *K. mikimotoi* (>200 cells mL^{-1}) was observed along east Johor Strait in 2011. Following the first occurrence of *K. mikimotoi* in Singapore waters, bloom patches of this dinoflagellate were subsequently detected in Punggol Marina and Changi Sailing Club (Leong *et al*., 2015). The observation in Changi Sailing Club recorded the cell densities of >5,000 cells mL^{-1} (Leong *et al*., 2015). The most recent bloom of *K. mikimotoi* in east Johor Strait, Singapore was observed in 2016, with the highest cell density exceeding 8,000 cells mL^{-1} (Kok & Leong, 2019). In Bolinao-Anda, Philippines, a very high abundance of K. mikimotoi were reported but no fish kill observed (Azanza & Benico, 2017). The increasing frequency and intensity of *K. mikimotoi* blooms in Southeast Asia is a continuous concern due to the adverse ecological impacts associated with this harmful dinoflagellate (Yñiguez *et al*., 2021).

Although there have been widespread occurrences of mass mortalities of aquatic animals globally, notably in Southeast Asia, there is no documented evidence of *K. mikimotoi* blooms in Malaysian waters. While *K. mikimotoi* blooms have not been reported in Malaysia, harmful algal bloom (HAB) monitoring on *K. mikimotoi* is crucial because this species has the potential to form harmful blooms that can lead to mass fish deaths and pose a serious threat to both marine life and aquaculture. Therefore, it is essential to collect scientific information to shed light on the presence of this harmful athecate dinoflagellate in Malaysia, particularly in the coastal waters of Borneo, as part of HAB monitoring. This study, thus, aims to document the occurrence of *K. mikimotoi* in Borneo, by opportunistic sampling in Sepanggar Bay, Sabah, Malaysian Borneo, followed by single cells isolation and culture establishment of the Kareniaceae-like cells. The clonal cultures were subsequently characterized by means of advanced morphological and molecular approaches. The species was identified based on the morphological traits examined through light and scanning electron microscopy, and further supported by molecular phylogenetic analysis of large subunit (LSU) and internal transcribed spacer (ITS) of the ribosomal RNA gene. The secondary structure of ITS2 transcript was modelled for *Karenia* species to infer the phylogenetic relationships. This study reports, for the first time, the detailed morphology and molecular characteristics of *K. mikimotoi* in Borneo's coastal waters.

MATERIALS & METHODS

Sampling Site and Algal Cultivation

Seawater samples were collected at Sepanggar Bay, Sabah (6°5'27.9" N 116°7'38.4" E) **(**Figure 1**)** using a 20-µm mesh-size plankton net and brought back to the laboratory for incubation. Single cell isolation (Hoshaw, 1973) from the seawater sample was carried out under light microscope Olympus BX51 (Olympus, Tokyo, Japan). The cells were grown in General-Purpose Medium (GPM) (Loeblich, 1975) and were kept in a temperature-controlled growth chamber at 25°C and light intensity of 100 µmol m^{-2} s^{-1} under a 12:12 h light:dark regime (Kon *et al.*, 2017). The culture established was deposited in the UNIMAS Harmful Algae Culture Collection with strain name KMSPBUD5.

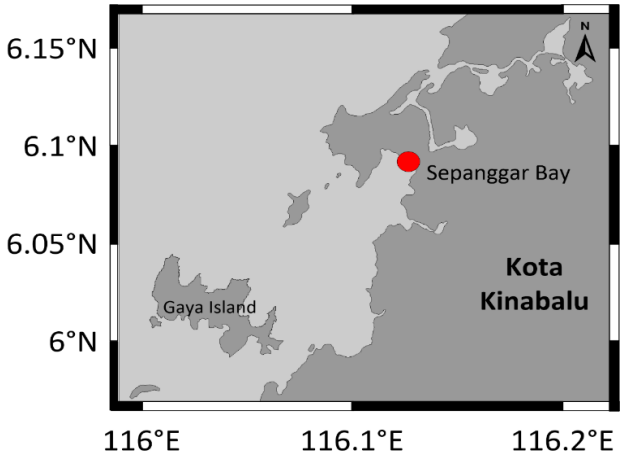

Figure 1. Map of Sabah, Malaysian Borneo showing the sampling site in this study

Light and Scanning Electron Microscopy

Live cells were examined under an Olympus BX51 light and fluorescence microscope (Olympus, Tokyo, Japan) to record the morphometric measurements, and positions of chloroplast and nucleus. Cells were stained with 0.1% SYBR Safe DNA stain (Invitrogen, MA, USA) to observe the nucleus under a fluorescence microscope using 450–490 nm excitation and 510–550 nm emission. For scanning electron microscopic observation, cells were fixed with 1% acidic Lugol's and 1% glutaraldehyde overnight (Nézan *et al*., 2014) and dehydrated in a graded ethanol series of 10%, 30%, 50%, 75%, 90%, 95%, and absolute ethanol. Samples were critical-point dried using the K850 Critical Point Dryer (Quorum, Laughton, United Kingdom), sputter-coated with gold palladium, and observed under a JEOL JSM-6510 Analytical Scanning Electron Microscope (JEOL, Tokyo, Japan).

DNA Extraction, Gene Amplification, Purification and Sequencing

Exponential-phased cells were harvested for genomic DNA extraction following the protocol of the DNeasy^{R} Plant Mini Kit (Qiagen, Hilden, Germany). The large subunit (LSU) of ribosomal RNA gene (rDNA) was amplified using the primer pair, D1R (5´–ACC CGC TGA ATT TAA GCA TA–3´) and D3Ca (5´–ACG AAC GAT TTG CAC GTC AG–3´) (Scholin *et al.*, 1994) The internal transcribed spacer (ITS) region was amplified using a primer pair designed *in silico* in this study, *viz.* SDINOITSF (5´–TCG TAA CAA GGT TTC CGT AGG TG–3´) and Smalldino ITS2R (5´–GGT ACT TGT TTG CTA TCG GTC TCG–3´).

For gene amplification using Polymerase Chain Reaction (PCR), 1× PCR buffer (Promega, Madison, WI, USA), 1.5 mM $MgCl^{2}$, 0.2 mM dNTPs (Qiagen, Hilden, Germany), 0.5 µM each primer, 2.5 U *Taq* DNA polymerase (Promega), and 10–100 ng μL^{-1} DNA were mixed in a 25 uL PCR cocktail. Gene amplification was performed in a Mastercycler® nexus GX2 thermocycler (Eppendorf, Hamburg, Germany). Gel electrophoresis was run at 75V for 25 min and illustrated in an E-Box gel documentation imaging (Vilber, Marne- la-Vallée, France). The amplicons were purified using the Promega Wizard® PCR Preps DNA Purification System (Madison, Wisconsin, United States) and Sanger sequencing were undertaken by Apical Scientific Sdn. Bhd. (Selangor, Malaysia).

Phylogenetic Analysis

Maximum Parsimony (MP), Maximum Likelihood (ML), and Bayesian Inference (BI) were used to infer the phylogenetic relationships between *K. mikimotoi* and its close relatives. PAUP* ver. 4.0b.10 (Swofford, 2003) was used for MP and ML runs. For the MP run, heuristic searches of 1,000 random-addition replications and branch-swapping with tree-bisection reconnection (TBR) were performed. Bootstrap analysis was performed with 1,000 bootstrap replications and 100 random sequence additions per bootstrap replicate. Heuristic searches and branch-swapping with 100 random addition replications in TBR were used for ML analysis. MrBayes 3 (Ronquist and Huelsenbeck, 2003) was used to run BI. The Akaike information criterion from jModelTest 2.1.10 (Darriba *et al*., 2012) was used to determine the best-fit model of ML and BI. FigTree v1.4.3 (Rambaut, 2007) was used to visualise the phylogenetic trees.

ITS2 Secondary Structure Modelling

ITS2 secondary structure of *Karenia* species was modelled from the ITS sequences based on the 5.8S–28S interaction identified at the proximal stem of the structure. The ITS2 secondary structure of *Karenia* species was predicted using the free energy minimization in RNAStructure v6.4 (Ali *et al*., 2023). The ITS2 RNA transcripts were modelled by homology modelling workflow (Wolf *et al.,* 2005), using the ITS2 Database (Koetschan *et al*., 2012; Merget *et al*., 2012). The ITS2 secondary structure was illustrated in VARNA (Darty *et al.,* 2009). The multiple sequence-structure alignment of *Karenia* ITS2 was generated in an ITS sequence structure-specific scoring matrix (Seibel *et al*., 2006) in 4SALE v1.7 (Seibel *et al*., 2006, 2008). The compensatory base change (CBC) and hemi-compensatory base change (hCBC) were identified in 4SALE (Wolf *et al*., 2005; Seibel *et al.*, 2006, 2008).

RESULTS

Morphological Characterisation of *K. mikimotoi*

The morphotype of *K. mikimotoi* was observed and identified in this study using single culture strain.

K. mikimotoi (Miyake & Kominami ex Oda) G. Hansen & Moestrup

Morphology: Cells are broadly ovoid, 22.1–27.4 µm long (25±1.6 µm; *n* = 30) and 17.2–23.9 µm wide (21±2.3 µm, *n* = 30). Cells are dorso-ventrally flattened, the epicone is conical and slightly smaller than the hemispherical hypocone, hypocone is with two lobes (Figure 2(a)–2(c)). The ellipsoidal nucleus is situated at the left side of the hypocone near the edge of cell, slightly extended into the epicone (Figure 2(d)–2(e)). The straight and wide apical groove is situated slightly above the sulcal intrusion extending to the dorsal of epicone, creating a slight indentation at the cell apex (Figure 2(a)–2(c), 2(f)–2(h)).

Locality: Sepanggar Bay (6°5’27.9” N 116°7’38.4” E), Sabah, Borneo, Malaysia

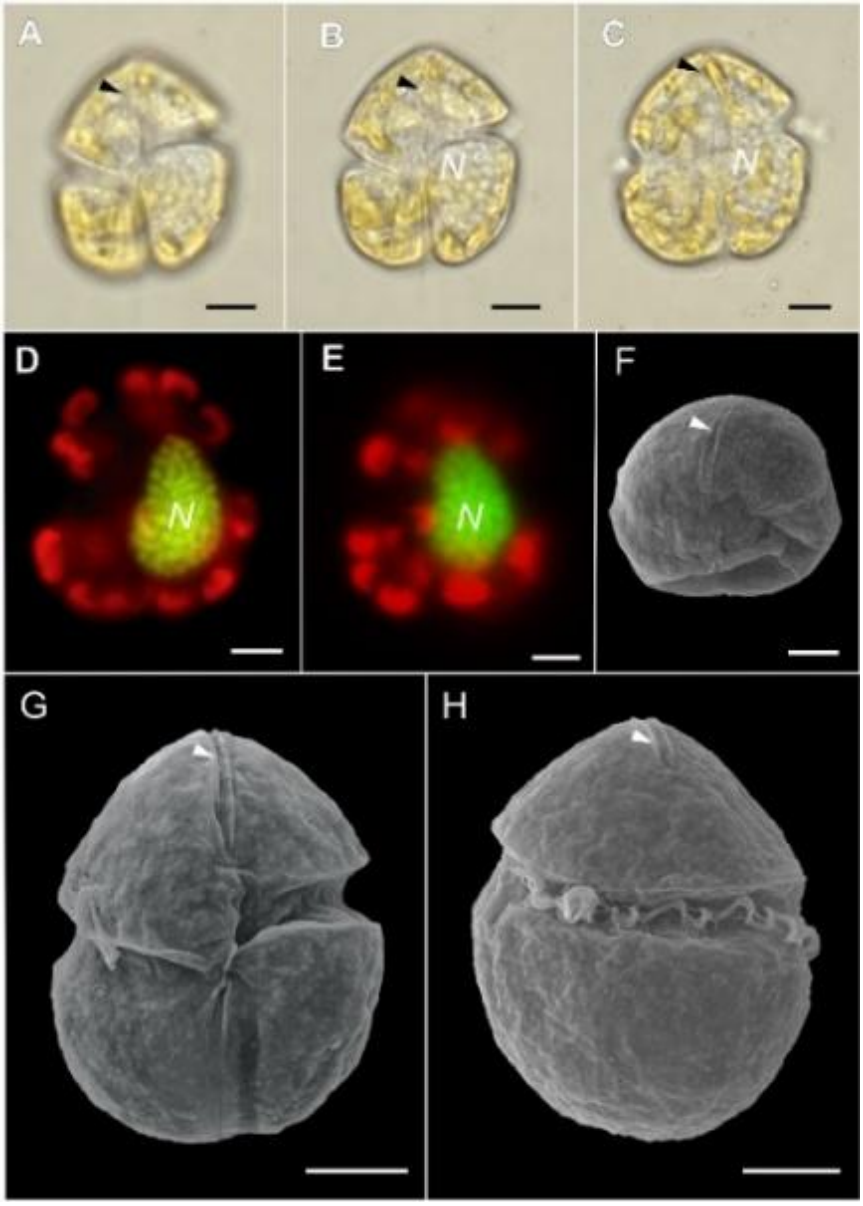

Figure 2. *Karenia mikimotoi*. (a-e) LM. Live cells showing apical groove (arrowhead) and nucleus (N). (d-e) SYBR Safe-stained cells with an ellipsoid nucleus (N) located on the left side of the hypocone nearing the edge of the cell. (f-h) SEM. Straight apical groove (arrowhead) in apical (f), ventral (g), and (h) dorsal views. Scales, 5 µm

Molecular Characterisation of *K. mikimotoi*

The LSU and ITS sequences of *K. mikimotoi* obtained in this study were deposited in the NCBI GenBank (LSU: PP993796 and ITS: PP993794). The D1–D3 region of the LSU and ITS rDNAs of *K. mikimotoi* were used to reconstruct the phylogenetic inferences of *Karenia* species. Similar tree topologies using MP, ML, and BI, were yielded from both phylogenetic trees, with the ML tree topologies showing the inferences (LSU, Figure 3; ITS, Figure 4). In the phylogenetic trees of this study, the *K. mikimotoi* from Sabah was notably positioned within a clade that included *K. mikimotoi* strains from previous studies. Both phylogenetic analyses revealed that *K. mikimotoi* formed a sister clade to *K. brevis* (ML bootstrap values/BI posterior probabilities, 100/100% in LSU tree, Figure 3; 94/99% in ITS tree, Figure 4). Grouping of *K. mikimotoi, K. brevis*, and *K. selliformis* was consistent in both LSU and ITS phylogenetic trees (Figure 3; Figure 4). The LSU tree (Figure 3) inferred monophyletic groups of (*K. selliformis, K. brevisulcata*, and *K. cristata*) (100/100%, Figure 3), and (*K. papilionacea, K. bidigitata* and *K. asterichroma*) (100/82%, Figure 3). In ITS tree (Figure 4), *K. selliformis, K. longicanalis* (synonym: *K. umbella*) and *K. aureolum* had formed a monophyletic clade (100/100%, Figure 4), which was paraphyletic to *K. papilionaceae* (100/100%; Figure 4). The molecular phylogenetic trees of this study also revealed the monophyletic clade of *Asterodinium gracile* and *K. papilionacea* (100/82%, Figure 3; 100/100%, Figure 4)., and the position of *Brachidinium capitatum* within the clade of *Karenia.*

ITS2 Secondary Structure of *Karenia*

ITS2 secondary structure of five *Karenia* species *viz. K. mikimotoi, K. brevis, K. selliformis, K. longicanalis* and *K. papilionaceae* were modelled. The ITS2 RNA transcripts of *Karenia* Clade I comprised of *K. mikimotoi, K. brevis* and *K. selliformis* (Figure 5), and *Karenia* Clade II consisted of *K. longicanalis* and *K. papilionaceae* (Figure 6). Comparison of the compensatory base changes (CBCs) and hemi-compensatory base changes (hCBCs) of *K. mikimotoi* to the closely related species were mapped on the transcripts. The pairwise structural comparison between *K. mikimotoi* and *K. brevis* (Figure 5) showed four hCBCs (in Helix I, G-U↔G-C; Helix II, A-C↔A-U, G-G↔G-U; Helix III, G-C↔G-U), and no CBC was detected. When comparing *K. mikimotoi* with *K. selliformis* (Figure 5), six hCBCs were revealed (in Helix I, G-U↔G-C, U-A↔U-C; Helix II, C-G↔G-G, A-C↔A-U; Helix III, G-C↔G-U, G-C↔A-C), no CBC was detected. When *K. brevis* was compared to *K. selliformis* (Figure 5), four hCBCs (in Helix I, U-A↔U-C; Helix II, C-G↔G-G, G-U↔G-C; Helix III, G-C↔A-C) and no CBC showed. Pairwise structural comparison of *K. longicanalis* and *K. papilionacea* (Figure 6) revealed three CBCs (in Helix IV, G-C↔U-G, A-U↔U-A, G-C↔A-U). The comparison of ITS2 RNA transcript of *K. longicanalis* and *K. papilionacea* (Figure 6) also showed ten hCBCs (in Helix I, U-G↔C-G, C-G↔U-G, U-G↔U-A; Helix II, C-G↔U-G; Helix III, U-G↔C-G, G-C↔G-U, G-C↔G-U, U-G↔C-G, G-U↔A-U, G-U↔A-U).

DISCUSSION

Morphology and Molecular Characterisation of *K. mikimotoi*

Cells of *K. mikimotoi* from Borneo coastal waters was within the similar size range as reported in previous studies of *K. mikimotoi* from distinct geographical region (Table 1). *K. mikimotoi* of Sabah was 22 to 27 µm long and 17 to 24 µm wide, and the cell sizes was within the range of previously reported *K. mikimotoi* which had cell sizes ranges between 20 and 38 µm long, 16 and 30 µm wide (Oda, 1935; Hansen *et al*., 2000; Haywood *et al*., 2004; Iwataki *et al*., 2022). Species of *Karenia* are morphologically variable but share common traits such as a dorso-ventrally flattened body, an elliptical or pentagonal cell shape, a straight apical groove, and sometimes an apical carina (Oda, 1935; Botes *et al*., 2003; de Salas *et al*., 2004; Haywood *et al*., 2004; Escobar-Morales & Hernández-Becerril, 2015; Hansen *et al*., 2000; Iwataki *et al*., 2022), and typically described having conical epicone and hemispherical hypocone (Oda, 1935; Haywood *et al*., 2004; Hansen *et al*., 2000; Iwataki *et al*., 2022). with key features including a straight apical groove on the epicone and no ventral pore (Daugbjerg *et al*., 2000).

Table 1. Morphological comparison of *Karenia mikimotoi* observed in this study and previous studies (n.d. = no data)

Reference(s)	In this study	Iwataki *et al.* (2022)	Hansen *et al.* (2000)	Oda (1935); Haywood *et al.* (2004)
Cell length (µm)	22.1–27.4 (25.0±1.6)	24.6–35.1 (31.2±3.0)	23.9–37.7 (32.8±3.4)	20.0–30.0 (24.8±0.4)
Cell width (µm)	17.2–23.9 (21.0±2.3)	21.9–30.9 (26.8±2.4)	21.6–36.4 (30.6±3.8)	16.0–30.0 (20.9±0.3)
Cell shape	Broadly ovoid and dorso-ventrally flattened, with conical epicone and two-lobed hemispherical hypocone	Conical epicone, hemispherical hypocone, dorsoventrally flattened	Conical or hemispherical epicone, hemispherical hypocone	Broadly ovoid and flattened dorsal abdomen, with wide conical epicone and two-lobed flakes hypocone
Nucleus	Ellipsoid, located on the left side of hypocone nearing the edge of cell	Round in the left hypocone, or ellipsoid in the left of the cell	Elongated, reniform or pyriform, situated in the left part of the cell	Ellipsoid, located on the left side of hypocone nearing the edge of cell
Sulcal intrusion	Present	Present, anterior was shallow and distal end was open	Present, narrow but widened slightly towards the antapex to slightly above epicone	Present at epicone
Ventral pore	Absent	n.d.	n.d.	n.d.
Apical groove	Straight, wide, slightly above sulcal intrusion extending to dorsal epicone	Straight	Delicate, narrow, situated to the left of sulcal axis extending from slightly above sulcal extension on the ventral side of cell way down the dorsal side of epicone	Straight, slightly above right side of the starting point of the sulcal intrusion extending to the dorsal epicone

Previous studies on *K. mikimotoi* (Oda, 1935; Haywood *et al*., 2004; Hansen *et al*., 2000; Iwataki *et al*., 2022) documented a visible apical groove, linear and narrow in shape that extended slightly above the sulcus intrusion to the dorsal side of the epicone. This is similar to the apical groove of *K. mikimotoi* observed in this study. Previous studies did not record the presence of a ventral pore (Oda, 1935; Hansen *et al*., 2000; Haywood *et al*., 2004; Iwataki *et al*., 2022), which was confirmed to be absent in *K. mikimotoi* as recorded in this study. The position of nucleus was one of the distinguishing characteristics for identifying *K. mikimotoi* (Tangen & Bjornland, 1981; Haywood *et al*., 2004; Wolny *et al*., 2024). A few studies had documented that the nucleus in *K. mikimotoi* was located at the left side of the cell (Hansen *et al*., 2000; Iwataki *et al*., 2022; Wolny *et al*., 2024). The position of nucleus of *K. mikimotoi* observed in this study was similar with the previous reports on this species.

The combination of morphological and molecular characterisation was utilized in this study to further support the species identification of *K. mikimotoi*. As an athecate dinoflagellate, *K. mikimotoi* is delicate and prone to deformation or even cell lysis during preservation (Krock *et al*., 2009). Therefore, the identification of

Karenia species often requires observation of live samples, as preserved samples may be ambiguous and make it difficult to obtain morphological features and morphometric data (de Salas *et al*., 2003; Bergholtz *et al*., 2006; Wayne *et al*., 2007). Identifying *K. mikimotoi* with microscope is challenging owing to its smaller cell size, minimal morphological divergence from other *Karenia* species under light microscope, and low cell abundance during non-bloom periods (Friedheim, 2016; Zhang *et al*., 2022). According to Haywood *et al*. (2004), microscopic identification of *K. mikimotoi* may be determined by cell size and nucleus position, while emphasises that molecular phylogenetic analysis is crucial in resolving difficulties in species identification. Molecular methods such as DNA sequencing of rDNA ITS and LSU region supports morphological data from light microscopy for more precise and reliable of species identification (Yuan *et al.*, 2012).

Molecular data not only aids in species delineation but also for facilitating comprehensive species characterisation and taxonomic classification (Monaco & Prouzet, 2015). *K. mikimotoi* is phylogenetically closer to *K. brevis*, and the results of this study agreed with past studies demonstrating the close relationship between *K. mikimotoi* and *K. brevis* (Ok *et al*., 2023). In addition, Benico *et al*. (2019) had documented *A. gracile* affinity to *K. papilionacea* and was closely related to *Karenia* species. The phylogenetic analysis in Henrichs *et al*. (2011) study had revealed the placement of *B. capitatum* in the *Karenia* clade. The placement of *A. gracile* and *B. capitatum* in the clade of genus *Karenia* was also revealed in this study and these findings had provided support for the inclusion of genera *Asterodinium* and *Brachidinium* in Kareniaceae family as reported in previous studies (Henrichs *et al*., 2011; Benico *et al*., 2019).

ITS2 Secondary Structure of *Karenia*

This study is the first to analyse and compare the ITS2 secondary structure of *Karenia* species to obtain a clearer understanding of the genetic relationships between species within this genus. The modelling of ITS2 secondary structures in *Karenia* revealed four highly conserved universal helices (I─IV). Helices I and IV are the most evolutionarily variable helices and are particularly useful for comparing species and subspecies, while helices II and III are more conserved in the lower taxonomic levels and differ from other eukaryotic ITS2 structures (Coleman, 2009).

In the molecular characterization of *K. mikimotoi*, *K. brevis*, and *K. selliformis*, phylogenetic analysis (Figure 3; Figure 4) reveals their separation into three distinct species lineages. This is further supported by the presence of hemi-compensatory base changes (hCBCs) when comparing their ITS2 transcripts (Figure 5). In a study on *Fukuyoa paulensis*, no compensatory base changes (CBCs) were detected among the clades, but an hCBC was observed in the most divergent clade (Laza-Martínez *et al*., 2016). In the present study, four hCBCs were identified between *K. mikimotoi* and *K. brevis* ITS2 transcripts, and six hCBCs were found in comparisons between *K. mikimotoi* and *K. selliformis* ITS2 transcripts (Figure 5). The presence of additional hCBCs increases genetic divergence between species, leading to their classification as separate species (Wolf *et al*., 2013). In other words, hCBCs play a crucial role in species divergence and represent a key step in speciation (Rousset *et al*., 1991; Wolf *et al*., 2013; Metzger *et al*., 2017). To further support the use of hCBCs as molecular markers in the ITS2 transcript, Teng *et al*. (2015) applied hCBCs to define new species identities in *Pseudo-nitzschia*.

Besides, based on ITS2 secondary structure and CBCs analyses *K. longicanalis* is distinct from *K. papilionaceae* by having three CBCs and ten hCBCs (Figure 6). Different species are more easily classified when CBCs are present in the homologous modelling of the ITS2 secondary structure (Coleman, 2003; Müller *et al*., 2007). The CBC information can be useful in evaluating species delineation, but divergence of ITS2 sequences due to hybridisation and polyploidisation can lead to misleading inferences of true homology between taxa and accurate phylogenetic reconstruction (Alvarez & Wendel, 2003). A good indicator of distinct species is the presence of at least one CBC (Müller *et al*., 2007; Wolf *et al*., 2013).

The taxa are classified as different species when CBCs or hCBCs are present in the homology modelling (Coleman, 2003; Müller *et al*., 2007). The predicted ITS2 secondary structure is sufficient to demarcate closely

related species, especially pseudo-cryptic and cryptic species (Amato *et al*.2007, Müller *et al*., 2007). In this study, the presence of hCBCs can be used as a diagnostic feature of species delineation in *Karenia* when CBCs are absent. The presence of CBCs or hCBCs of ITS2 transcript in this study can serve as supporting information in species delimitation among *Karenia* species.

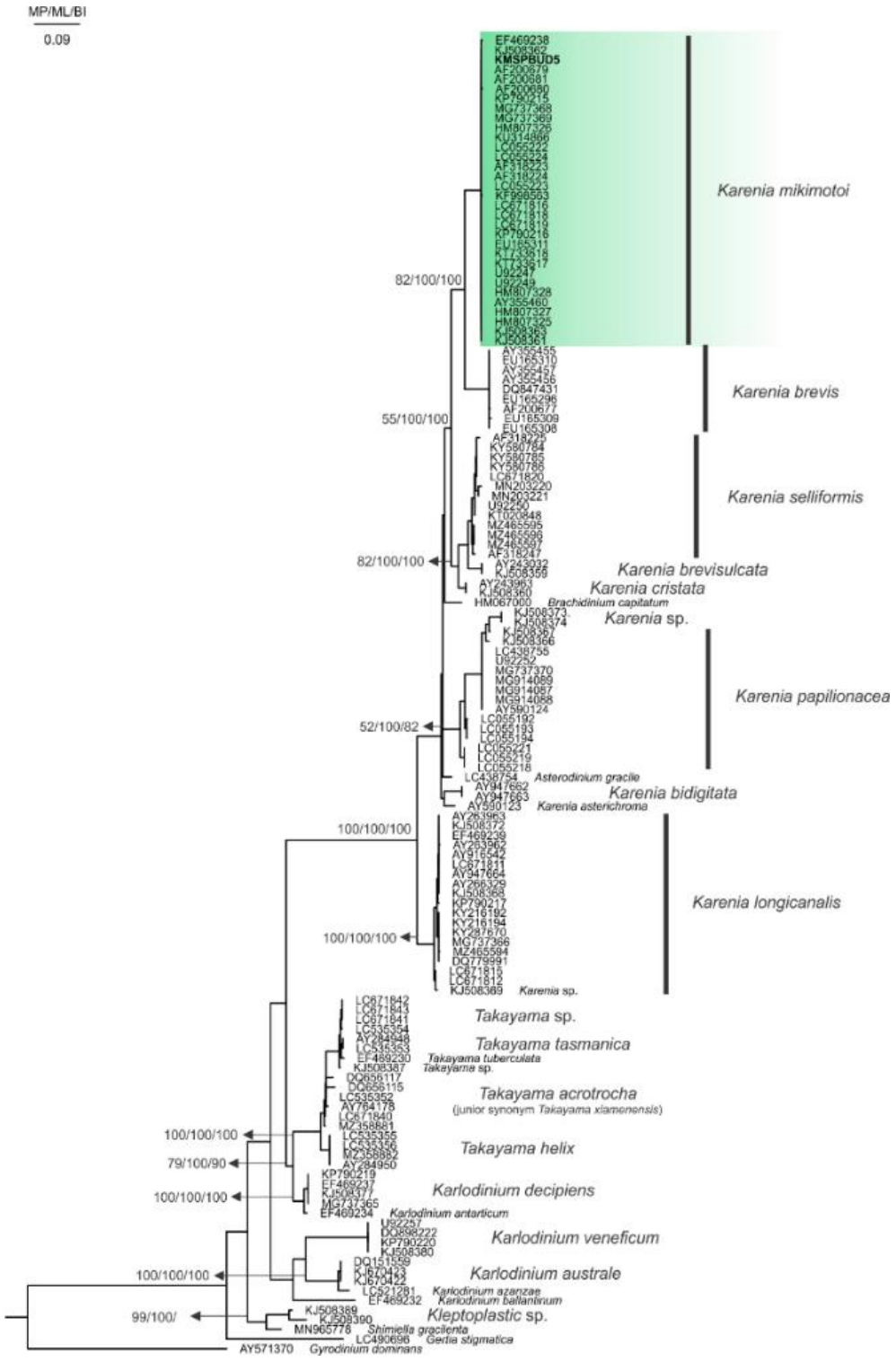

Figure 3. Phylogeny tree inferred from maximum likelihood (ML) based on *Karenia* LSU rDNA datasets. Nodal supports are bootstrap values of maximum parsimony (MP), maximum likelihood (ML), and posterior probability of BI; only values >50% support are indicated. The studied species are in bold. *Gyrodinium dominans* was chosen as the outgroup

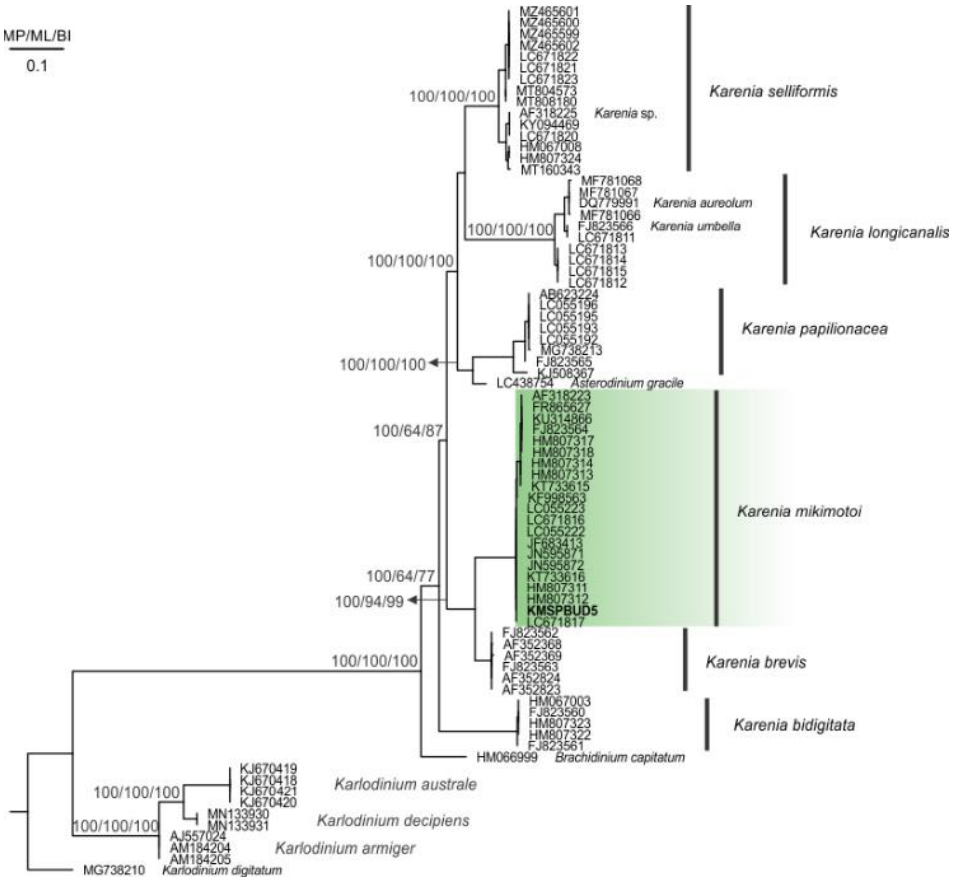

Figure 4. Phylogeny tree inferred from maximum likelihood (ML) based on *Karenia* ITS rDNA datasets. Nodal supports are bootstrap values of maximum parsimony (MP), maximum likelihood (ML), and posterior probability of BI; only values >50% support are indicated. The studied species are in bold. *Karlodinium digitatum* was chosen as the outgroup

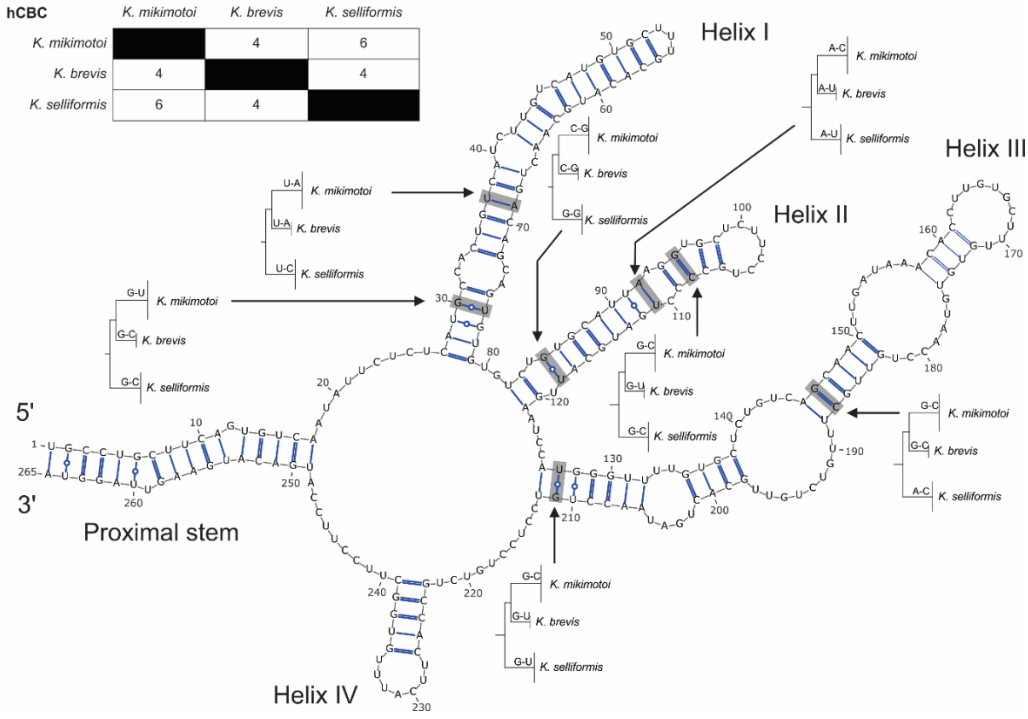

Figure 5. ITS2 RNA transcripts of *Karenia mikimotoi* with closely related species, viz. *Karenia brevis* and *Karenia selliformis.* Shaded rectangles indicate hCBCs

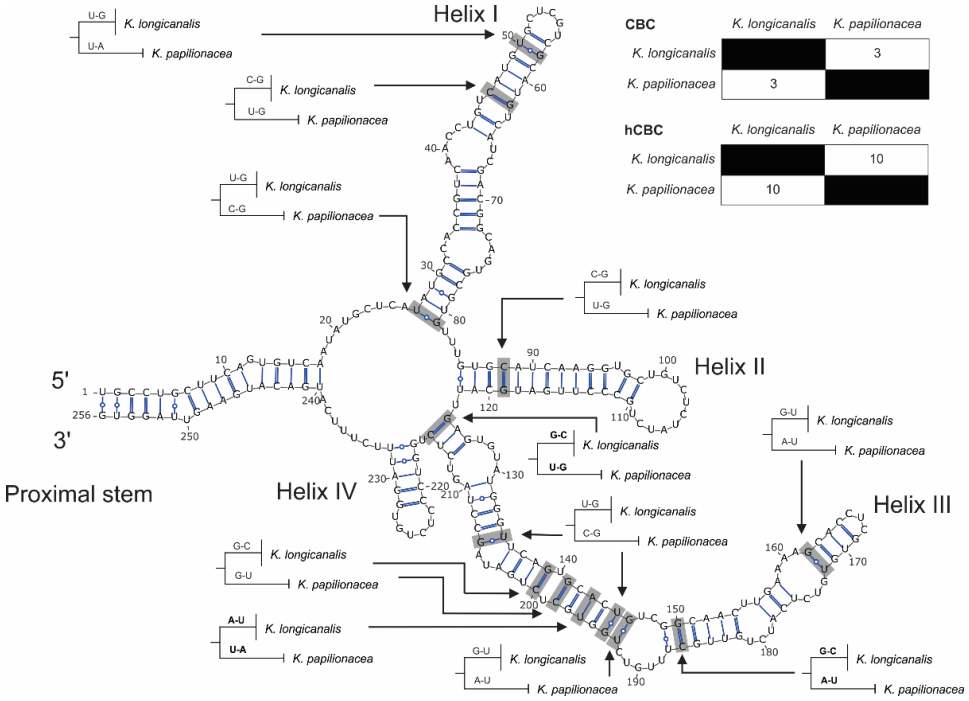

Figure 6. ITS2 RNA transcripts of *Karenia longicanalis* with closely related species, viz. *Karenia papilionacea*. Shaded rectangles indicate CBCs or hCBCs. Bolded indicate CBCs

Geographical Distribution and Bloom Events of *K. mikimotoi* in Asia

The bloom-forming dinoflagellate species *K. mikimotoi* has been documented in temperate coastal waters along the coasts of Atlantic, Pacific, and Indian Oceans (Li *et al*., 2019). Although *K. mikimotoi* is documented for the first time in Borneo coastal waters in this study, it has a long history of widespread distribution with detrimental impacts on marine life in other Asian countries, for instances, Japan, China, Singapore, Vietnam, Korea and India. First report of *K. mikimotoi* was during red tides in 1934 in Japan, where this toxic species was associated with fish and shellfish kills along the shore of Gokasho Bay, Honshu (Oda, 1935). Since then, *K. mikimotoi* was reported to bloom from 1991 to 1995 in several areas in Japan, including Tanabe Bay, Hoketsu Bay, Suo-Nada, near Ie-shima islands, and Hiroshima Bay (Nakamura *et al*., 1995; Koizumi *et al*., 1996; Kimura *et al*., 1999; Matsuyama *et al*., 1999). Among all the affected countries, China is the most affected by the blooms of *K. mikimotoi*. The first discovery of *K. mikimotoi* in China dates back to 1998 in Daya Bay and the Pearl River estuary (Baohong *et al*., 2021). Since then, *K. mikimotoi* blooms have recurred over 120 times in China, becoming an annual calamity even in current 21st century (Baohong *et al*., 2021; Zhang *et al*., 2023). The longest period of *K. mikimotoi* bloom recorded in China was in the Yangtze River estuary, lasting for 72 days in 2006 (Baohong *et al*., 2021). In 2012, 22 blooms of *K. mikimotoi* were observed affecting Zhejiang Province, Fujian Province, and Guangdong Province (Baohong *et al*., 2021). *K. mikimotoi* has also been documented in several Southeast Asian countries, including Singapore (Leong *et al*., 2015; Kok & Leong, 2019) and Vietnam (Larsen & Nguyen, 2004). Park *et al*. (2013) documented the occurrence of *K. mikimotoi* on the Geoje coast of Korea. In India, *K. mikimotoi* blooms were linked to fish kills along the Kerala coast in 2004 (D'Silva *et al*., 2012), Cochin Barmouth in 2009 (Hartman *et al*., 2014), Gulf of Mannar in 2013 (Babu *et al*., 2016), and Kochi estuary (Kumar *et al*., 2018). The distribution of *K. mikimotoi* is believed to be facilitated by ballast water carried by international vessels. A study by Wang *et al*. (2010, as cited in Wang *et al*., 2022) linked the movement and subsequent invasion of *K. mikimotoi* into new regions of the China Sea to ballast water transport, highlighting the role of shipping in the spread of this species. The detection of *K. mikimotoi* in Sabah, especially near the international port at Sepanggar Bay, Kota Kinabalu, further highlights its extensive distribution via ballast water.

Table 2. Summary of red-tides attributed to *K. mikimotoi* in Asia with detrimental effects to marine life (n.d. = no data)

Year	Area	Adverse effects	Reference
1934	Japan; Gokasho Bay, Honshu	Fish, shellfish mortality Fish gills disorder, mucus spawn	Oda (1935)
1965	Japan; Omura Bay, Nagasaki	Fish, shellfish mortalities	Takayama and Adachi (1984)
1972	Japan; Omura Bay, Nagasaki	n.d.	Hirayama (1972); Gentien (1998)
1981	Korea; Geoje coast	n.d.	Park *et al.* (2013)
1985	Japan; Suo-Nada and Iyo-Nada	Fisheries damage >10 million US$	Yanagi *et al.* (1995)
1989	India; Kodi, Karnataka	Fish mortality	D'Silva *et al.* (2012)
1991	Japan; Tanabe Bay	n.d.	Nakamura *et al.* (1995)
1992	Japan; Hoketsu Bay	n.d.	Koizumi *et al.* (1996)
1992	Japan; Suo-Nada	n.d.	Kimura *et al.* (1999)
1993	Japan; Suo-Nada	n.d.	Kimura *et al.* (1999)
1994	Japan; near Ie-shima Islands	n.d.	Nakamura *et al.* (1995)
1995	Japan; Hiroshima Bay	Shellfish mortality	Matsuyama *et al.* (1999)
1998	China; Pearl River estuary and Daya Bay	Fish mortality	Dickman (2000); Qi *et al.* (2004)
2002	China; Fujian coast	Fish, shellfish mortalities	Li *et al.* (2017)
2003	China; East China Sea coast	n.d.	Li *et al.* (2017)
2003	China; Zhejiang Province	n.d.	Baohong *et al.* (2021)
2004	China; Tianjin and Yellow River estuary	n.d.	Baohong *et al.* (2021)
2004	China; Bohai Sea and East China Sea	n.d.	Li *et al.* (2017)
2004	India; Kerala coast	Fish mortality	D'Silva *et al.* (2012)
2004	Vietnam coast	n.d.	Larsen and Nguyen (2004)
2005	China; Yangtze River estuary, Bohai Bay and Zhejiang Province	n.d.	Baohong *et al.* (2021)
2005	China; East China Sea coast and Pearl River estuary	Fish, shellfish mortalities	Li *et al.* (2009); Li *et al.* (2010); Li *et al.* (2017)
2006	China; East China Sea coast	n.d.	Li *et al.* (2017)
2006	China; Yangtze River estuary and Zhejiang Province	n.d.	Baohong *et al.* (2021)
2007	China; Bohai Sea and East China Sea	n.d.	Li *et al.* (2017)
2008	China; East China Sea coast	n.d.	Li *et al.* (2017)
2008	Japan; Suo-Nada and Beppu Bay	Fish mortality	Siswanto *et al.* (2013)
2009	China; East China Sea coast	n.d.	Li *et al.* (2017)
2009	India; Cochin barmouth	Fish mortality	Hartman *et al.* (2014)
2010	China; East China Sea coast	n.d.	Li *et al.* (2017)
2010	Japan; Beppu Bay	n.d.	Siswanto *et al.* (2013)
2011	Singapore; Johor Straits	n.d.	Leong *et al.* (2015)
2012	China; East China Sea coast	Abalone, fish mortalities	Li *et al.* (2017)
2012	China; Zhejiang Province and Fujian Province	n.d.	Baohong *et al.* (2021)
2013	India; Gulf of Mannar	Fish mortality	Babu *et al.* (2016)
2014	Singapore; Johor Straits	n.d.	Leong *et al.* (2015)
2014	Japan; Imari Bay	n.d.	Aoki *et al.* (2017)
2014	China; East China Sea coast	n.d.	Li *et al.* (2019)
2015	Japan; Hakodate Bay	Abalone, fish, squid mortalities	Shimada *et al.* (2016)
2015	China; East China Sea coast	n.d.	Li *et al.* (2019)
2015	Japan; Sasebo Bay	n.d.	Higo *et al.* (2017)
2015	India; Kochi estuary	n.d.	Kumar *et al.* (2018)
2017	China; Zhejiang Province	n.d.	Baohong *et al.* (2021)
2017	Philippines; Bolinao-Anda, Pangasinan	High abundance yet no fish kill reported	Azanza and Benico (2017); Yñiguez *et al*., 2021
2018	China; East China Sea coast	Fish, abalone mortality	Li *et al.* (2019)
2022	Malaysia; Sabah, Borneo	n.d.	This study

CONCLUSION

In this study, we discovered *K. mikimotoi*, for the first time, in Malaysia Borneo. This suggests the prevalence of this toxic athecate dinoflagellate in our waters that require attention for monitoring of HABs in Malaysia. Therefore, further studies on the diversity and distribution of *Karenia* in Malaysia are recommended to determine the diversity and distribution of *Karenia* in Malaysia as well as to assess the potential risk of toxic dinoflagellate *Karenia* occurrence especially in finfish and shellfish mariculture area in the country.

ACKNOWLEDGEMENTS

We would like to acknowledge the Universiti Malaysia Sarawak for supports and this work was funded by the Ministry of Higher Education, Malaysia, Fundamental Research Grant Scheme (FRGS) (FRGS/1/2020/WAB11/UNIMAS/03/2). This work forms parts of the master project of Sheryl Uncha anak Andrew Chiba.

REFERENCES

Ali, S.E., Mittal, A. & Mathews, D.H. (2023). RNA secondary structure analysis using RNAstructure. *Current Protocols, 3,* e846. DOI: 10.1002/cpz1.846

Amato, A., Kooistra, W.H., Ghiron, J.H., Mann, D.G., Pröschold, T., & Montresor, M. (2007). Reproductive isolation among sympatric cryptic species in marine diatoms. *Protist, 158*(2), 193–207. DOI: 10.1016/j.protis.2006.10.001

Azanza, R.V. & Benico, G.A. (2017). "Fish kills" in the Philippines associated with harmful algal blooms (HABs). *Proceedings of the Tenth EASTHAB Symposium.*

Babu, M.J., Geetha, P. & Soman, K.P. (2016). MODIS-aqua data based detection and classification of algal blooms along the coast of India using RLS classifier. *Procedia Computer Science, 93,* 424-430. DOI: 10.1016/j.procs.2016.07.238

Baohong, C., Kang, W., Huige, G. & Hui, L. (2021). *Karenia mikimotoi* blooms in coastal waters of China from 1998 to 2017. *Estuarine, Coastal and Shelf Science, 249,* 107034. DOI: 10.1016/j.ecss.2020.107034

Benico, G., Takahashi, K., Lum, W.M. & Iwataki, M. (2019). Morphological variation, ultrastructure, pigment composition and phylogeny of the star-shaped dinoflagellate *Asterodinium gracile* (Kareniaceae, Dinophyceae). *Phycologia, 5*(4), 405-418. DOI: 10.1080/00318884.2019.1601948

Bergholtz, T., Daugbjerg, N. & Fernández, M. (2006). On the identity of *Karlodinium veneficum* and description of *Karlodinium armiger* sp. nov. (*Dinophyceae*), based on light and electron microscopy, nuclear-encoded LSU rDNA, and pigment composition. *Journal of Phycology, 42,* 170-193. DOI: 10.1111/j.1529-8817.2006.00187.x

Botes, L., Sym, S. & Pitcher, G. (2003). *Karenia cristata* sp. nov. and *Karenia bicuneiformis* sp. nov. (*Gymnodiniales, Dinophyceae*): two new *Karenia* species from the South African Coast. *Phycologia, 42,* 563-571. DOI: 10.2216/i0031-8884-42-6-563.1

Caruana, A. M. N. & Amzil, Z. (2018). Chapter 13 - Microalgae and Toxins. In: Microalgae in Health and Disease Prevention (Levine, I. A. and Fleurence, J., 1st ed.), pp. 263-305. London: Academic Press.

Cen, J., Wang, J., Huang, L., Ding, G., Qi, Y., Cao, R., Cui, L. & Lü, S. (2020). Who is the "murderer" of the bloom in coastal waters of Fujian, China, in 2019? *Journal of Oceanology and Limnology, 38,* 722-732. DOI: 10.1007/s00343-020-9290-8

Cen, J., Lu, S., Moestrup, Ø., Jiang, T., Ho, K. C., Li, S., Li, M., Huan, Q. & Wang, J. (2024). Five *Karenia* species along the Chinese coast: with the description of a new species, *Karenia hui* sp. nov. (Kareniaceae, Dinophyta). *Harmful Algae, 137,* 102645. DOI: 10.1016/j.hal.2024.102645

Coleman, A.W. (2003). ITS2 is a double-edged tool for eukaryote evolutionary comparisons. *Trends in Genetics, 19,* 370-375. DOI: 10.1016/S0168-9525(03)00118-5

Coleman, A.W. (2009). Is there a molecular key to the level of "biological species" in eukaryotes? A DNA guide. *Molecular Phylogenetics and Evolution, 50,* 197-203. DOI: 10.1016/j.ympev.2008.10.008

D'Silva, M.S., Anil, A.C., Naik, R.K. & D'Costa, P.M. (2012). Algal blooms: a perspective from the coasts of India. *Natural Hazards, 63,* 1225-1253. DOI: 10.1007/s11069-012-0200-3

Darriba, D., Taboada, G.L., Doallo, R. & Posada, D. (2012). jModelTest 2: more models, new heuristics and parallel computing. *Nature Methods, 9,* 772. DOI: 10.1038/nmeth.2109

Darty, K., Denise, A., & Ponty, Y. (2009). VARNA: Interactive drawing and editing of the RNA secondary structure. *Bioinformatics, 25*(15), 1974–1975. DOI: 10.1093/bioinformatics/btp250

Daugbjerg, N., Hansen, G., Larsen, J. & Moestrup, Ø. (2000). Phylogeny of some of the major genera of dinoflagellates based on ultrastructure and partial LSU rDNA sequence data, including the erection of three new genera of unarmoured dinoflagellates. *Phycologia, 39*, 302-317. DOI: 10.2216/i0031-8884-39-4-302.1

Davis, C.C. (1948). *Gymnodinium brevis* sp. nov., a cause of discolored water and animal mortality in the Gulf of Mexico. *Botanical Gazette, 109*, 358-360. DOI: 10.1086/335561

de Salas, M.F., Bolch, C.J.S., Botes, L., Nash, G., Wright, S.W. & Hallegraeff, G.M. (2003). *Takayama* gen. nov. (Gymnodiniales, Dinophyceae), a new genus of unarmored dinoflagellates with sigmoid apical grooves, including the description of two new species. *Journal of Phycology, 39*, 1233-1246. DOI: 10.1111/j.0022-3646.2003.03-086.x

de Salas, M.F., Bolch, C.J.S. & Hallegraeff, G. M. (2004). *Karenia umbella* sp. nov. (Gymnodiniales, Dinophyceae), a new potentially ichthyotoxic dinoflagellate species from Tasmania, Australia. *Phycologia, 43*, 166-175. DOI: 10.2216/i0031-8884-43-2-166.1

Ericson, K. (2016). Making space for red tide: discoloured water and the early twentieth century bayscape of Japanese pearl cultivation. *Journal of the History of Biology, 50*, 393-423. DOI: 10.1007/s10739-016-9443-x

Escobar-Morales, S. & Hernández-Becerril, D. (2015). Free-living marine planktonic unarmoured dinoflagellates from the Gulf of Mexico and the Mexican Pacific. *Botanica Marina, 58*, 9-22. DOI: 10.1515/bot-2014-0084

Eunson, R. (1955). *The Pearl King: The Fabulous Story of Mikimoto.* New York: Greenberg.

Flewelling, L.J., Naar, J.P., Abbott, J.P., Baden, D.G., Barros, N.B., Bossart, G.D., Bottein, M.-Y.D., Hammond, D.G., Haubold, E.M., Heil, C.A., Henry, M.S., Jacocks, H.M., Leighfield, T.A., Pierce, R.H., Pitchford, T.D., Rommel, S.A., Scott, P.S., Steidinger, K.A., Truby, E.W., Van Dolah, F.M. & Landsberg, J.H. (2005). Red tides and marine mammal mortalities. *Nature, 435*, 755-756. DOI: 10.1038/nature435755a

Friedheim, S. (2016). Comparison of species identification methods: DNA barcoding versus morphological taxonomy. *Journal of Microbiology & Experimentation, 3*(1), 00082. DOI: 10.15406/jmen.2016.03.00082

Fukuyo, Y., Imai, I., Kodama, M. & Tamai, K. (2002). Red tides and other harmful algal blooms in Japan. In: Taylor, F. J. R. and Trainer, V. L. (eds.) *Harmful algal blooms in the PICES region of the North Pacific.* Sidney, B.C., Canada: Institute of Ocean Sciences.

Gentien, P. (1998). Bloom dynamics and ecophysiology of the *Gymnodinium mikimotoi* species complex. *Physiological ecology of harmful algal blooms*, 155-173.

Guiry, M.D. & Guiry, G.M. (2023). AlgaeBase. World-wide electronic publication. Available: https://www.algaebase.org.

Gunter, G., Williams, R.H., Davis, C.C. & Smith, F.G.W. (1948). Catastrophic mass mortality of marine animals and coincident phytoplankton bloom on the West Coast of Florida, November 1946 to August 1947. *Ecological Monographs, 18*, 309-324. DOI: 10.2307/1948622

Hansen, G., Daugbjerg., N. & Henriksen, P. (2000). Comparative study of *Gymnodinium mikimotoi* and *Gymnodinium aureolum*, comb. nov. (=*Gyrodinium* aureolum) based on morphology, pigment composition, and molecular data. *Journal of Phycology*, 36(2), 394-410. DOI: 10.1046/j.1529-8817.2000.99172.x

Hartman, S.E., Hartman, M.C., Hydes, D.J., Smythe-Wright, D., Gohin, F., & Lazure, P. (2014). The role of hydrographic parameters, measured from a ship of opportunity, in bloom formation of Karenia mikimotoi in the English Channel. *Journal of Marine Systems*, 139: 455-463. DOI: 10.1016/j.jmarsys.2014.07.001

Haywood, A.J., Steidinger, K.A., Truby, E.W., Bergquist, P.R., Bergquist, P.L., Adamson, J. & Mackenzie, L. (2004). Comparative morphology and molecular phylogenetic analysis of three new species of the genus *Karenia* (Dinophyceae) from New Zealand. *Journal of Phycology, 40*(1), 165-179. DOI: 10.1111/j.0022-3646.2004.02-149.x

Heil, C.A. & Steidinger, K.A. (2009). Monitoring, management, and mitigation of *Karenia* blooms in the eastern Gulf of Mexico. *Harmful Algae, 8*, 611-617. DOI: 10.1016/j.hal.2008.11.006

Henrichs, D.W., Olson, R.J., Sosik, H.M. & Campbell, L. (2011). Phylogenetic analysis of *Brachidinium capitatum* (Dinophyceae) from the Gulf of Mexico indicates membership in the Kareniaceae. *Journal of Phycology*, *47*(2), 366-374. DOI: 10.1111/j.1529-8817.2011.00960.x

Hoagland, P., Jin, D., Polansky, L.Y., Kirkpatrick, B., Kirkpatrick, G., Fleming, L.E., Reich, A., Watkins, S.M., Ullmann, S.G. & Backer, L.C. (2009). The costs of respiratory illnesses arising from Florida gulf coast *Karenia brevis* blooms. *Environmental Health Perspectives*, *117*(8), 1239–1243. DOI: 10.1289/ehp.0900645

Hoshaw, R.W. (1973). Methods for microscopic algae. *Handbook of phycological methods: culture methods***,** 53-68.

Hulburt, E.M. (1957). The taxonomy of unarmored Dinophyceae of shallow embayments on Cape Cod, Massachusetts. *The Biological Bulletin, 112,* 196-219. DOI: 10.2307/1539198

Iwataki, M., Lum, W.M., Kuwata, K., Takahashi, K., Arima, D., Kuribayashi, T., Kosaka, Y., Hasegawa, N., Watanabe, T., Shikata, T., Isada, T., Orlova, T.Y. & Sakamoto, S. (2022). Morphological variation and phylogeny of *Karenia selliformis* (Gymnodiniales, Dinophyceae) in an intensive cold-water algal bloom in eastern Hokkaido, Japan. *Harmful Algae, 114*, 102204. DOI: 10.1016.j.hal.2022.102204

Kimura, B., Kamizono, M., Etoh, T., Koizumi, Y., Murakami, M. & Honjo, T. (1999). Population development of the red tide dinoflagellate *Gymnodinium mikimotoi* in inshore waters of Japan. *Plankton Biology and Ecology, 46*(1), 37-47.

Koetschan, C., Hackl, T., Müller, T., Wolf, M., Förster, F. & Schultz, J. (2012). ITS2 database IV: interactive taxon sampling for internal transcribed spacer 2 based phylogenies. *Molecular Phylogenetics and Evolution*, 63: 585–588.

Koizumi, Y., Uchida, T. & Honjo, T. (1996). Diurnal vertical migration of *Gymnodinium mikimotoi* during a red tide in Hoketsu Bay, Japan. *Journal of Plankton Research*, *18*(2), 289-294. DOI: 10.1093/plankt/18.2.289

Kok, J.W.K. & Leong, S.C.Y. (2019). Nutrient conditions and the occurrence of a *Karenia mikimotoi* (Kareniaceae) bloom within East Johor Straits, Singapore. *Regional Studies in Marine Science, 27,* 100514. DOI: 10.1016/j.rsma.2019.100514

Kon, N.F., Lau, W.L.S., Hii, K.S., Law, I.K., Teng, S.T., Lim, H.C., Takahashi, K., Gu, H., Lim, P.T. & Leaw, C.P. (2017). Quantitative real-time PCR detection of a harmful unarmoured dinoflagellate, *Karlodinium australe* (Dinophyceae). *Phycological Research, 65***,** 291-298. DOI: 10.1111/pre.12186

Krock, B., Pitcher, G., Ntuli, J. & Cembella, A. (2009). Confirmed identification of gymnodimine in oysters from the west coast of South Africa by liquid 145 chromatography-tandem mass spectrometry. *African Journal of Marine Science, 31,* 113-118. DOI: 10.2989/AJMS.2009.31.1.12.783

Kumar, P.S., Kumaraswami, M., Rao, G.D., Ezhilarasan, P., Sivasankar, R., Rao, V.R. & Ramu, K. (2018). Influence of nutrient fluxes on phytoplankton community and harmful algal blooms along the coastal waters of southeastern Arabian Sea. *Continental Shelf Research, 161*, 20-28. DOI: 10.1016/j.csr.2018.04.012

Larsen, J. & Nguyen, N.L. (2004). Potentially toxic microalgae of Vietnamese waters. *Opera Botanica, 140*, 5-216.

Laza-Martínez, A., David, H., Riobó, P., Miguel, I. & Orive, E. (2016). Characterization of a Strain of *Fukuyoa paulensis* (Dinophyceae) from the Western Mediterranean Sea. *Journal of Eukaryotic Microbiology, 63*(4), 481–497. DOI: 10.1111/jeu.12292

Li, X., Yan, T., Lin, J., Yu, R. & Zhou, M. (2017). Detrimental impacts of the dinoflagellate *Karenia mikimotoi* in Fujian coastal waters on typical marine organisms. *Harmful Algae*, 61, 1-12. 137. DOI: 10.1016/j.hal.2016.11.011

Li, X., Yan, T., Yu, R. & Zhou, M. (2019). A review of *Karenia mikimotoi*: Bloom events, physiology, toxicity and toxic mechanism. *Harmful Algae, 90*, 101702. DOI: 10.1016/j.hal.2019.101702

Loeblich, A. R. (1975). A seawater medium for dinoflagellates and the nutrition of *Cachonina niel*. *Journal of Phycology*, *11***,** 80-86. DOI: 10.1111/j.1529-8817.1975.tb02752.x

Leong, S., Yew, C., Peng, L. L., Moon, C. S., Kit, J. K. W. & Ming, S. T. L. (2015). Three new records of dinoflagellates in Singapore's coastal waters, with observations on environmental conditions associated with microalgal growth in the Johor Straits. *Raffles Bulletin of Zoology, 31,*24-36.

Matsuyama, Y., Uchida, T. & Honjo, T. (1999). Effects of harmful dinoflagellates, *Gymnodinium*

mikimotoi and *Heterocapsa circularisquama*, red-tide on filtering rate of bivalve molluscs. *Fisheries Science*, *65*, 248-253. DOI: 10.2331/fishsci.65.248

Merget, B., Koetschan, C., Hackl, T., Förster, F., Dandekar, T., Müller, T., Schultz, J., & Wolf, M. (2012). The ITS2 Database. *Journal of Visualized Experiments*, (61), 3806. DOI: 10.3791/3806

Metzger, B.P.H., Wittkopp, P.J. & Coolon, J.D. (2017). Evolutionary dynamics of regulatory changes underlying gene expression divergence among *Saccharomyces* species. *Genome Biology and Evolution*, *9*(4), 843-854. DOI: 10.1093/gbe/evx035

Monaco, A. & Prouzet, P. (2015). *Marine Ecosystems: Diversity and Functions.* Wiley.

Müller, T., Philippi, N., Dandekar, T., Schultz, J., & Wolf, M. (2007). Distinguishing species. *RNA*, *13*(9), 1469–1472. DOI: 10.1261/rna.617107

Nakamura, Y., Suzuki, S. & Hiromi, J. (1995). Population dynamics of heterotrophic dinoflagellates during a *Gymnodinium mikimotoi* red tide in the Seto Inland Sea. *Marine Ecology Progress Series*, *125*, 269-277.

Nézan, E., Siano, R., Boulben, S., Six, C., Bilien, G., Chèze, K., Duval, A., Le Panse, S., Quéré, J. & Chomérat, N. (2014). Genetic diversity of the harmful family Kareniaceae (Gymnodiniales, Dinophyceae) in France, with the description of *Karlodinium gentienii* sp. nov.: A new potentially toxic dinoflagellate. *Harmful Algae, 40***,** 75-91. DOI: 10.1016/j.hal.2014.10.006

Oda M. (1935). The red tide of *Gymnodinium mikimotoi* n.sp. (MS.) and the effect of altering copper sulphate to prevent the growth of it. *Zoological Society of Japan*, *47*(555): 35-48.

Ok, J.H., Jeong, H.J., Lim, A.S., Kang, H.C. You, J.H., Park, S.A. & Eom, S.H. (2023). Lack of mixotrophy in three *Karenia* species and the prey spectrum of *Karenia* mikimotoi (Gymnodiniales, Dinophyceae). *Algae*, *38*(1), 39-55. DOI: 10.4490/algae.2023.38.2.28

Park, J., Jeong, H.J., Yoo, Y.D. & Yoon, E.Y. (2013). Mixotrophic dinoflagellate red tides in Korean waters: distribution and ecophysiology. *Harmful Algae*, *30*, S28-S40. DOI: 10.1016/j.hal.2013.10.004

Partensky, F., Vaulot, D., Couté, A. & Sournia, A. (1988). Morphological and nuclear analysis of the bloom-forming dinoflagellates *Gyrodinium* cf. *aureolum* and *Gymnodinium nagasakiense*. *Journal of Phycology*, *24*(3), 408-415. DOI: 10.1111/j.1529-8817.1988.tb04484.x

Rambaut, A. (2007). FigTree, a graphical viewer of phylogenetic trees.

Ronquist, F. & Huelsenbeck, J.P. (2003). MrBayes 3: Bayesian phylogenetic inference under mixed models. *Bioinformatics*, *19*, 1572-1574. DOI: 10.1093/bioninformatics/btg180

Ronquist, F., Teslenko, M., van der Mark, P., Ayres, D.L., Darling, A., Höhna, S., Larget, B., Liu, L., Suchard, M.A. & Huelsenbeck, J.P. (2012). MrBayes 3.2: efficient Bayesian phylogenetic inference and model choice across a large model space. *Systematic Biology*, *61*, 539-542. DOI: 10.1093/sysbio/sys029

Rousset, F., Pélandakis, M. & Solignac, M. (1991). Evolution of compensatory substitutions through G-U intermediate state in Drosophila rRNA. *Proceedings of the National Academy of Sciences of the United States of America*, *88*, 10032-10036. DOI: 10.1073/PNAS.88.22.10032.

Seibel, P.N., Müller, T., Dandekar, T., Schultz, J. & Wolf, M. (2006). 4SALE – a tool for synchronous RNA sequence and secondary structure alignment and editing. *Bioinformatics*, *7*(498). DOI: 10.1186/1471-2105-7-498

Seibel, P.N., Müller, T., Dandekar, T. & Wolf, M. (2008). Synchronous visual analysis and editing of RNA sequence and secondary structure alignments using 4SALE. *BMC Research Notes*, *1*(91). DOI: 10.1186/1756-0500-1-91

Seibel, P., Müller, T., Dandekar, T. & Wolf, M. (2008). Synchronous visual analysis and editing of RNA sequence and secondary structure alignments using 4SALE. *BMC Research Notes*, 1: 91.

Siswanto, E., Ishizaka, J., Tripathy, S.C. & Miyamura, K. (2013). Detection of harmful algal blooms of *Karenia mikimotoi* using MODIS measurements: a case study of Seto-Inland Sea, Japan. *Remote Sensing of Environment*, *129*, 185-196. DOI: 10.1016/j.rse.2012.11.012

Swofford, D.L. (2003). PAUP* Phylogenetic Analysis Using Parsimony (*and Other Methods). Version 4. http://paup.csit.fsu.edu/.

Takayama, H. & Adachi, R. (1984). *Gymnodinium nagasakiense* sp. nov., a red-tide forming

dinophyte in the adjacent waters of Japan. *Bulletin of Plankton Society of Japan, 31,* 7-14.

Tangen, K. (1977). Blooms of *Gyrodinium aureolum* (Dinophygeae) in North European waters, accompanied by mortality in marine organisms. *Sarsia, 63,* 123-133. DOI: 10.1080/00364827.1977.10411330

Tangen, K. & Bjornland, T. (1981). Observations on pigments and morphology of *Gyrodinium aureolum* Hulburt, a marine dinoflagellate contain 19'hexanoyloxyfucoxantin as the main carotenoid. *Journal of Plankton Research, 3,* 389-401. DOI: 10.1093/plankt/3.3.389

Tang, Y.Z., Egerton, T.A., Kong, L. & Marshall, H.G. (2008). Morphological variation and phylogenetic analysis of the dinoflagellate *Gymnodinium aureolum* from a tributary of Chesapeake Bay. J. Eukaryot. Microbiol. 55, 91–99. DOI: 10.1111/j.1550-7408.2008.00305.x

Teng, S.T., Lim, P.T., Lim, H.C., Rivera-Vilarelle, M., Quijano-Scheggia, S., Takata, Y., Quilliam, M.A., Wolf, M., Bates, S.S. & Leaw, C.P. (2015). A non-toxigenic but morphologically and phylogenetically distinct new species of *Pseudo-nitzschia*, *P. sabit* sp. nov. (Bacillariophyceae). *Journal of Phycology, 51,* 706-725. DOI: 10.1111/jpy.12318

Wang, Q., Lin, L., Chen, X., Wu, W. & Wu, H. (2022). Transportation of bloom forming species in ballast water by commercial vessels at Yangshan deep water port. *Ocean and Coastal Management, 219,* 106045. DOI: 10.1016/j.ocecoaman.2022.106045

Watkins, S.M.A.R., Fleming, L.E. & Hammond, R. (2008). Neurotoxic shellfish poisoning. *Marine Drugs, 6,* 431-455. DOI: 10.3390/md20080022

Wayne, L.R., Vandersea, M.W., Kibler, S.R., Reece, K.S., Stokes, N.A., Lutzoni, F. M., Yonish, B.A., West, M.A., Black, M.N.D. & Tester, P.A. (2007). Recognizing dinoflagellate species using ITS rDNA sequences. *Journal of Phycology, 43,* 344-355. DOI: 10.1111/j.1529-8817.2006.00305.x

Wolf, M., Achtziger, M., Schultz, J., Dandekar, T., & Müller, T. (2005). Homology modeling revealed more than 20,000 rRNA internal transcribed spacer 2 (ITS2) secondary structures. *RNA, 11*(11), 1616–1623. DOI: 10.1261/rna.2144205

Wolf, M., Chen S., Song, J., Ankenbrand, M., & Müller, T. (2013). Compensatory base changes in ITS2 secondary structures correlate with the biological species concept despite intragenomic variability in ITS2 sequences - a proof of concept. *PLoS One, 8*(6), e66726. DOI: 10.1371/journal.pone.0066726

Wolny, J.L., Whereat, E.B., Egerton, T.A., Gibala-Smith, L.A., McKay, J.R., O'Neil, M., Wazniak, C.E. & Mulholland, M.R. (2024). The occurrence of *Karenia* species in mid-Atlantic coastal waters:data from the Delmarva Peninsula, USA. *Harmful Algae, 132,* 102579. DOI: 10.1016/j.hal.2024.102579

Yanagi, T., Yamamoto, T., Koizumi, Y., Ikeda, T., Kamizono, M. & Tamori, H. (1995). A numerical simulation of red tide formation. *Journal of Marine Systems, 6,* 269-285. DOI: 10.1016/0924-7963(94)00030-K

Yñiguez, A.T., Lim, P.T., Leaw, C.P., Jipanin, S.J., Iwataki, M., Benico, G. & Azanza, R.V. (2021). Over 30 years of HABs in the Philippines and Malaysia: what have we learned? *Harmful Algae, 102,* 101776. DOI: 10.1016/j.hal.2021.101776

Yuan, J., Mi, T., Zhen, Y., & Yu, Z. (2012). Development of a rapid detection and quantification method of *Karenia mikimotoi* by real-time quantitative PCR. *Harmful Algae, 17,* 83-91.DOI: 10.1016/J.HAL.2012.03.004

Zhang, W., Zhang, Q., Smith, K.F., Qiu, L., Liu, C., Yin, X. & Liu, Q. (2022). Development of specific DNA barcodes for the Dinophyceae family Kareniaceae and their application in the South China Sea. *Frontiers in Marine Science, 9.* DOI: 10.3389/fmars.2022.851605

Zhang, Y., Song, X. & Zhang, P. (2023). Combined effects of toxic *Karenia mikimotoi* and hypoxia on the juvenile abalone *Haliotis discus hannai*. *Journal of Shellfish Research, 42*(2), 373-379. DOI: 10.2983/035.042.0207